

## A Sum Frequency Generation Study of the Room-Temperature Ionic Liquid–Titanium Dioxide Interface

Cesar Aliaga and Steven Baldelli\*

Department of Chemistry, University of Houston, Houston, Texas 77204-5003

Received: October 5, 2007; In Final Form: December 4, 2007

The interfacial structure between TiO<sub>2</sub> and the room-temperature ionic liquids 1-butyl-3-methylimidazolium dicyanamide ([BMIM][DCA]) and 1-butyl-3-methylimidazolium methyl sulfate ([BMIM][MS]) was examined using sum frequency generation (SFG) vibrational spectroscopy and contact angle measurements. Vibrations corresponding to the normal modes of the [BMIM]<sup>+</sup> cation and dicyanamide [DCA]<sup>−</sup> were detected. The results suggest that the cation and the anion are present and oriented at the interface for [BMIM][DCA]. The molecular orientation of the ionic species was calculated using a simulation on the basis of the polarization dependence of the sum frequency spectra. The tilt of the C<sub>3</sub> axis of the methyl group from the butyl chain in [BMIM]<sup>+</sup> ranges from 57 to 90° from the surface normal for [BMIM][MS] and from 66 to 90° for [BMIM][DCA]. The C<sub>2</sub> axis from the dicyanamide anion tilts at an angle of 53–90° as a function of the twist. The imidazolium ring seems to lie nearly parallel to the TiO<sub>2</sub> surface as suggested by the SFG spectra, contact angle results, and surface charge density calculations. Finally, specific adsorption of [DCA]<sup>−</sup> was also observed, in contrast to a weak adsorption of [MS]<sup>−</sup>. The enhance charge adsorption could explain the efficiency of these compounds in dye-sensitized solar cells.

### Introduction

Among the various applications of room-temperature ionic liquids is their role as alternative electrolyte materials in several electrochemical devices such as batteries,<sup>1–4</sup> fuel cells,<sup>5,6</sup> double-layer capacitors,<sup>7–10</sup> and photoelectrochemical solar cells.<sup>11–16</sup> Dye-sensitized TiO<sub>2</sub> solar cells are the most intensively investigated devices, since the development of the Grätzel cell, which provided a high light-to-electric energy conversion yield.<sup>17</sup> The principle of these devices lies in the fact that when photons, carrying an energy greater than the band gap of the active medium, strike a semiconductor, electron/hole pairs are created, which can generate an electric potential at a junction of two different materials. Solar cells based on dye-sensitized mesoporous titanium dioxide are low cost alternatives to the traditional solid-state devices, which are often made of doped forms of crystalline or amorphous silicon, where the absorption of light and the transport of charge carriers are not two separate processes.<sup>17–20</sup> In dye-sensitized solar cells, photon energy conversion to electricity is achieved by electron injection from a photoexcited dye into the conduction band of a semiconductor, followed by dye regeneration and hole transport to a counter electrode to complete the electrical circuit. The dye-sensitized porous semiconductor (TiO<sub>2</sub>) is immersed in an electrolyte containing a I<sub>3</sub><sup>−</sup>/I<sup>−</sup> redox couple that mediates the dye regeneration process by hole injection into the hole-transport medium, which varies depending on the type of cell. For the regenerative cell type, the holes are scavenged by a reduced redox molecule, which migrates to the other electrode and is reduced by the electrons. The solid/liquid interface thus plays a crucial role, which is the reason the semiconductor electrode is usually composed by mesoporous TiO<sub>2</sub> in order to increase the surface area.<sup>15,18,19</sup>

Traditionally, dye-sensitized solar cells use organic solvents such as acetonitrile in the constitution of the electrolyte, to which

inorganic ions are added to provide conductivity. However, organic solvents have some limitations such as flammability and evaporation under warm temperatures, or reactivity, which causes stability issues. That is why imidazolium-based room-temperature ionic liquids were investigated as electrolytes, due to their nonvolatility, relatively high conductivity, and low viscosity. Furthermore ionic liquids contribute to the enhancement of the photovoltaic performance of the devices by increasing of conductivity of the I<sup>−</sup>/I<sub>3</sub><sup>−</sup> electrolyte, as evidenced by the improvement of the diffusion coefficient.<sup>11,13,21,22</sup>

This study focuses on the investigation of the ionic liquid/TiO<sub>2</sub> interface for the ionic liquids [BMIM][DCA] and [BMIM][MS] by means of sum frequency generation vibrational spectroscopy. The relevance of the study lies in the growing importance that solar energy conversion acquired in the last decades, a field whose technical applicability was renewed with the development of dye-sensitized solar cells. The system under study is an important component in solar devices, since interfacial processes play a critical role in the light conversion process. An understanding at the molecular level of the structure of the interface is therefore central.<sup>19,20</sup>

The investigation aims to detect the ionic species present at the solid–liquid boundary and to determine the molecular orientation of the functional groups to acquire a better description of that interface. The choice of the cation is relevant since imidazolium cations are essential to the high performance of ionic liquids in dye-sensitized solar cells.<sup>21</sup> The anions in this investigation, [DCA]<sup>−</sup> and [MS]<sup>−</sup>, are important because dicyanamide-based ionic liquids have been used in dye-sensitized solar cells to improve the conversion efficiency, which is due to the lower viscosity that dicyanamide confers to the ionic liquids it forms.<sup>15,23,24</sup> In addition, those ions produce well-defined vibrational spectra, which allows for a detailed analysis, and a comparison may be established between alkyl-containing and simple inorganic anions.

The ionic liquid/TiO<sub>2</sub> interface has recently been the topic of molecular modeling and molecular dynamic simulations.<sup>25,26</sup> From these simulations and comments therein by Gratzel, the high charge density of the ionic liquid allows for efficient screening of the surface charging thus preventing a charge build up and allowing for the efficient electron transfer at high irradiance. This situation demonstrates that the ionic liquids are much more effective at screen electric field at the surface than normal electrolyte solutions. The use of the ionic liquids as a conducive media allows the solar cell to operate much more efficiently; however the details on the surface structure and organization at the solid/liquid surface are not known experimentally. The SFG results here present a molecular level description of this system.

## Experimental Section

**Sum Frequency Generation (SFG).** SFG is a nonlinear optical spectroscopy sensitive only in noncentrosymmetric environments such as gas–liquid, solid–liquid, and liquid–liquid interfaces.

In the SFG experimental setup, two laser beams of frequencies  $\omega_1$  and  $\omega_2$  overlap at the surface of a nonlinear medium and generate a nonlinear polarization  $P^{(2)}(\omega_1+\omega_2)$  described by

$$P^{(2)} = \chi^{(2)}:EE \quad (1)$$

where  $E$  is the electric field of the incoming laser beam and  $\chi^{(2)}$  is the second-order nonlinear susceptibility. The intensity of the SFG signal is proportional to the square of the absolute value of  $P^{(2)}$ .  $\chi^{(2)}$  has nonresonant and resonant terms,  $\chi_{NR}$  and  $\Sigma\chi_R^{(2)}$ , respectively.  $\chi_{NR}$  is a background effect from the interface, and  $\Sigma\chi_R^{(2)}$  includes contributions from individual resonant modes  $\chi_R^{(2)}$ . The expression for  $\chi_R^{(2)}$  is

$$\chi_R^{(2)} = \left( \frac{N\langle\beta^{(2)}\rangle}{\omega_{IR} - \omega_q + i\Gamma_q} \right) \quad (2)$$

where  $N$  is the number of modes contributing to the SFG signal,  $\Gamma_q$  is the damping constant for the  $q$ th vibrational mode with a frequency  $\omega_q$ ,  $\omega_{IR}$  is the frequency of the incoming IR beam, and  $\langle\beta^{(2)}\rangle$  is the molecular hyperpolarizability averaged over all possible molecular orientations and contains the Raman polarizability and the IR dipole transition moment. It is evident that whenever  $\omega_q$  becomes comparable to  $\omega_{IR}$ ,  $\chi_R^{(2)}$  becomes large, resulting in a peak in the SFG spectrum.<sup>27–29</sup>

**Materials.** The ionic liquids used in this study were synthesized according to literature methods,<sup>30–33</sup> and the synthetic procedure and purification were described in earlier publications from this group for [BMIM][DCA]<sup>34</sup> and [BMIM][MS].<sup>35</sup> The structures of both compounds are shown in Figure 1.

### Sample Preparation for the Sum Frequency Spectroscopy.

The purified ionic liquid sample is filtered through a fine sintered glass frit and then is vacuum-dried overnight in a separate vessel equipped with O-ring fittings, at approximately 40 °C and until  $5 \times 10^{-5}$  Torr is reached, while stirring. It is then pressurized with dry argon previous to the transfer into the SFG cell.

The solid–liquid SFG cell is made of Pyrex and was home-built (Figure 2). It consists of a vacuum O-ring fitting with one end closed flat and two O-ring fitting terminated high-vacuum valves attached to the sides. The valves have Teflon stopcocks fitted with O-rings. All the O-rings that come in contact with the ionic liquid are made of Kalrez. A TiO<sub>2</sub>-coated calcium fluoride window is attached and sealed to the top fitting with a

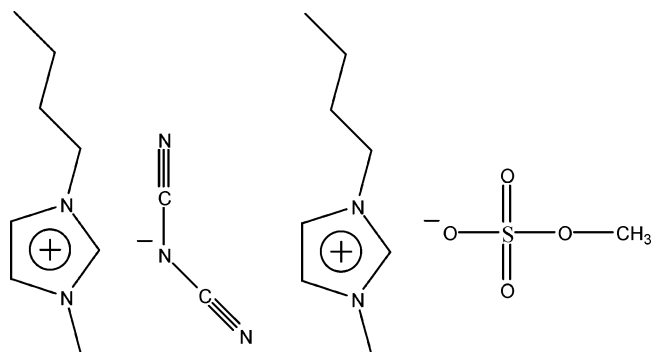


Figure 1. Structures of [BMIM][DCA] (left) and [BMIM][MS] (right).

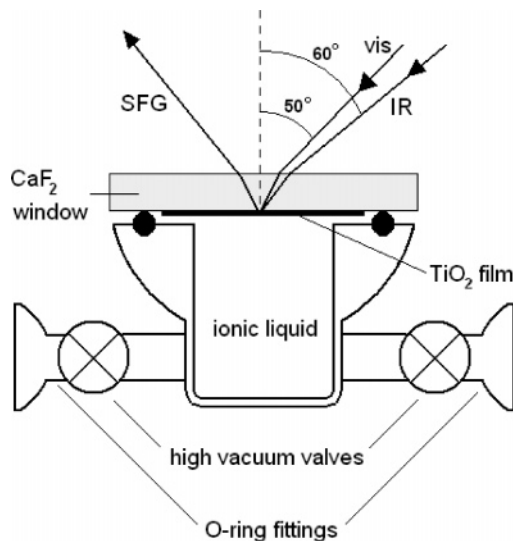
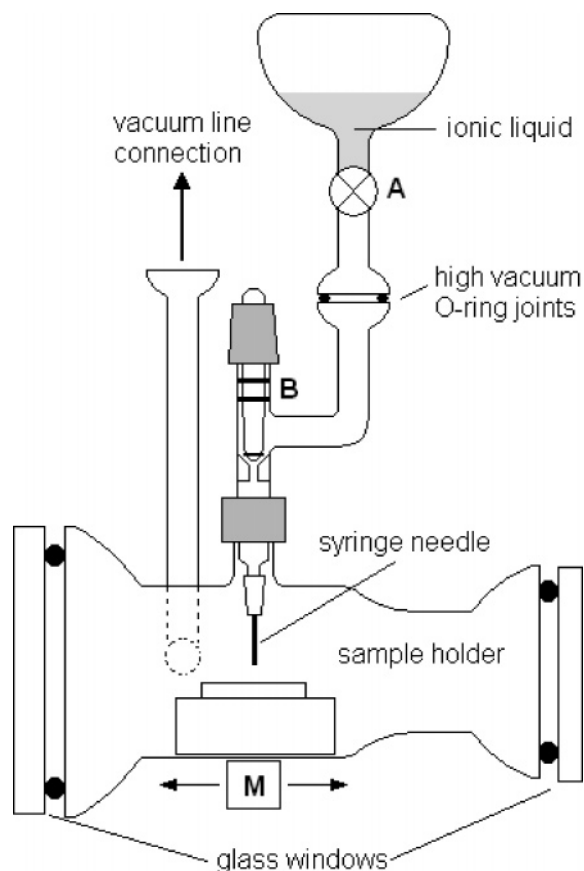


Figure 2. Diagram of the solid/liquid SFG cell.

Kalrez O-ring. The cell is able to hold a vacuum to a pressure of  $10^{-5}$  Torr. The TiO<sub>2</sub> window was prepared by deposition of TiO<sub>2</sub> nanoparticles on a CaF<sub>2</sub> window by Shultz's group at Tufts University. The average size of the nanoparticles is 2.4 nm, and they belong to the anatase phase.<sup>36</sup>

Before introduction of the sample into the cell, the glass body is cleaned in a 50/50 mixture of nitric acid/sulfuric acid mixture for several hours, rinsed with deionized water, and baked at 570 °C. The stopcocks and Kalrez O-rings are boiled in a solution of Micro 90 and subsequently boiled several times with deionized water. The window is rinsed with deionized water and then irradiated with a high-intensity UV lamp (ILC technologies) for 1 h, to photooxidize adsorbed organic matter, and finally rinsed again.<sup>37</sup> The absence of adsorbed organic matter was tested with transmission FTIR (Thermo Nicolet Avatar 360 FT-IR). Other investigators have confirmed the oxidation of adsorbed organic matter on TiO<sub>2</sub> by UV irradiation. SFG spectra before and after irradiation show the complete removal of the organic species.<sup>37–40</sup> Additional work on the removal of adsorbed organic matter under UV irradiation on TiO<sub>2</sub> used water contact angle measurements, confirming the induced hydrophilicity of the oxide.<sup>41</sup> In this study, the induced hydrophilicity was tested qualitatively and the results are similar to those in the literature.

The cell is then assembled and evacuated for 2 h to a pressure of  $5 \times 10^{-5}$  Torr. Finally, the ionic liquid is airless transferred to the evacuated cell through O-ring fitting connections to avoid any contamination from the atmosphere.



**Figure 3.** Scheme of the contact angle measurement cell. M = magnet (to immobilize the sample holder), B = dosing valve, and A = vessel valve.

#### Sample Preparation for the Contact Angle Measurements.

For the measurement of contact angles, the liquid sample is prepared the same way as for the sum frequency experiment. After being dried in a separate vessel down to a pressure of  $5 \times 10^{-5}$  Torr, a small portion of ionic liquid is airless transferred to the contact angle measurement cell, which was designed and built in this research laboratory (see Figure 3). The cell is made of Pyrex glass and is terminated by two O-ring joints that seal against two glass windows with Viton O-rings. It is also equipped with two additional connections, one for the evacuation of the cell and the other is attached to a compression fitting that holds the syringe needle and valve system. The transfer is performed under vacuum, and for this purpose, stopcock valve B is initially open while keeping valve A closed to evacuate the entire cell. This is performed until the cell reaches the base pressure. Subsequently, valve A is opened as to allow just a few drops to be delivered. The amount of liquid sent to the syringe tip is controlled by valve B, so that only one drop falls on the  $\text{TiO}_2$  surface. The sample holder consists of a half Teflon cylinder and contains an embedded magnet. It is therefore susceptible to manipulation by an external magnet M to correctly position the substrate before the drop falls and to keep the sample holder steady during the process. The sample ( $\text{TiO}_2$  film) is prepared as described above. The measurement is performed using a digital Exwave HAD Sony camera, and the images are processed using ImageJ software, with a plug-in by Stalder.<sup>42</sup>

**Spectroscopy System.** The spectroscopy setup was described previously.<sup>34</sup> It consists of an EKSPLA PL2143A/20 picosecond pulsed Nd:YAG laser with a 25 ps pulse and a 20 Hz repetition rate, whose 1064 nm output pumps an optical parametric generation/amplification system (LaserVision OPG/OPA). The

OPG/OPA system produces an infrared beam tunable from 2000 to 4000  $\text{cm}^{-1}$  and a fixed 532 nm beam. The visible and the IR beams are collimated and overlap at the surface of the sample in copropagating geometry, with angles (with respect to the surface normal) of  $50^\circ$  for the visible and  $60^\circ$  for the IR. The available energy densities at the region where the beams overlap are 20.4  $\text{mJ}/\text{cm}^2$  for the 532 nm beam and 55.4 and 22.4  $\text{mJ}/\text{cm}^2$  for the infrared beam from 2879 to 2100  $\text{cm}^{-1}$ , respectively. The SFG signal is then collected by a photomultiplier tube (Hamamatsu R3788), and sent to a gated integrator. A computer program collects it and averages it over five scans of 20 shots/point at 1  $\text{cm}^{-1}/\text{s}$ .

**Data Collection and Analysis.** The frequency of the IR laser beam is scanned at a rate of 1  $\text{cm}^{-1}/\text{s}$ . Each data point corresponds to 20 averaged laser shots. Five spectra/polarization combination are obtained, and the average is plotted along with error bars. The data are corrected for fluctuations in the infrared beam, and any IR absorption by the system is taken into account by dividing the averaged spectrum by the signal of a reference channel, which is obtained by overlapping the reflected infrared beam with a portion of the incoming 532 nm beam on a film of a nonlinear compound such as barium titanate. The reference signal is collected and detected using a separate monochromator and PMT. The resulting SFG spectra are then curve fitted using eq 5, and the subsequently extracted peak amplitudes and widths are used in the orientation calculations.

**Orientation Analysis.** The orientation of the cation and anion is derived from the polarization dependence of the sum frequency spectra. The procedure is similar to that of Hirose et al.<sup>43–45</sup> and Wang et al.,<sup>46,47</sup> who use the bond additivity model as an approximation. The terminal methyl groups of the alkyl chains are assigned  $C_{3v}$  symmetry and possess free rotation around the  $C_3$  symmetry axis, therefore having an orientation described by the tilt of the axis. The dicyanamide ion is assigned  $C_{2v}$  symmetry, but no free rotation is assumed around its symmetry axis and it has therefore a tilt angle  $\theta$  and a twist angle  $\phi$ .

The principle of polarization dependence compares the ratio of peak intensities of different vibrational modes with theoretical curves of peak intensity ratio versus orientational angle. Expressions for the kinetic energy matrix elements necessary for the calculation of the hyperpolarizabilities were obtained from the calculation of the hyperpolarizabilities were obtained from the rigorous derivation method were applied.  $[\text{DCA}]^-$  was assigned  $C_{2v}$  symmetry, and the  $G$  matrix elements for the antisymmetric and symmetric  $\text{C}\equiv\text{N}$  stretches were obtained and subsequently used in the hyperpolarizability expressions.<sup>43</sup> More details on the normal-mode analysis can be found in a previous publication.<sup>48</sup>

Simulation curves of peak intensity ratios versus tilt angle,  $\theta$ , as a function of the orientational distribution width,  $\sigma$ , or the twist angle,  $\phi$ , were constructed and plotted simultaneously with the experimental peak ratios obtained from the fits of the spectra. A Gaussian expression was adopted for the distribution.<sup>49,50</sup> From such analysis, a range of possible tilt angles for the symmetry axis of the chemical group under analysis with respect to the surface normal was obtained.

## Results

**Spectroscopy. [BMIM][DCA].** The C–H vibrations were probed in the 2750–3300  $\text{cm}^{-1}$  interval, and the  $\text{C}\equiv\text{N}$  modes, in the 2000–2300  $\text{cm}^{-1}$  frequency interval. The spectra for the anion are shown in Figure 4 for polarizations ssp and ppp, since ssp and pss combinations show almost no features. The spectra

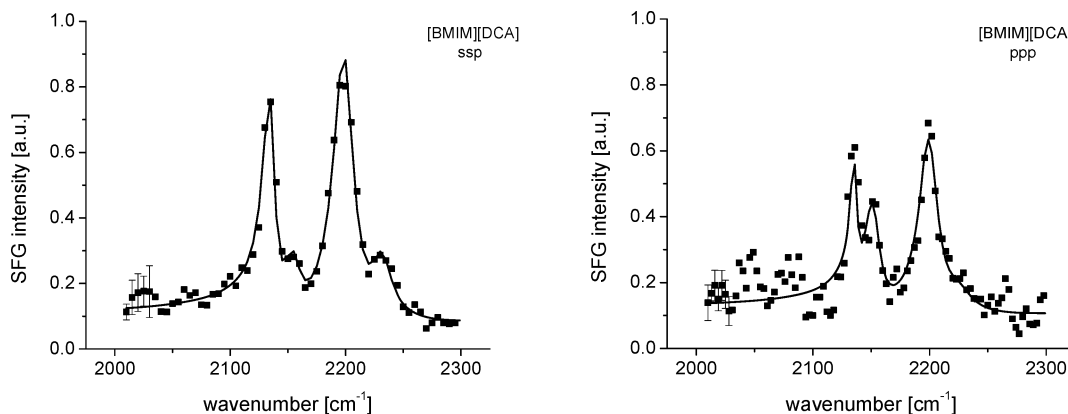


Figure 4. SFG spectra of [BMIM][DCA]/TiO<sub>2</sub> interface in the CN stretch region for polarizations ssp and ppp.

TABLE 1: SFG Vibrational Spectroscopy Results for [BMIM][DCA] and [BMIM][MS]<sup>a</sup>

bond	type	[BMIM][DCA]				[BMIM][MS]			
		ssp	ppp	sps	pss	ssp	ppp	sps	pss
C–H	r <sup>+</sup>	2878	2883	n/p	n/p	2880	2883	n/p	n/p
	r <sup>+</sup> <sub>FR</sub>	2945	n/p	n/p	n/p	2945	n/p	n/p	n/p
	r <sup>-</sup>	n/p	2966	2969	2970	n/p	2966	2969	2970
	d <sup>+</sup>	2852	s/n	s/n	s/n	2852	s/n	s/n	s/n
	d <sup>-</sup>	n/p	2902	2899	2899	n/p	n/p	2903	2900
	d <sup>+</sup> <sub>FR</sub>	2918	n/p	n/p	n/p	2924	2917	n/p	n/p
ss C <sub>4</sub> –C <sub>5</sub>		3172	3177	n/p	n/p	3204	n/p	n/p	n/p
	as C <sub>4</sub> –C <sub>5</sub>	3132	3111	n/p	n/p	3112	n/p	n/p	n/p
C≡N	as C≡N	2135	2136	s/n	s/n	n/a	n/a	n/a	n/a
	ss C≡N	2199	2200	s/n	s/n	n/a	n/a	n/a	n/a
	isonitrile <sup>b</sup>	2155	2152	s/n	s/n	n/a	n/a	n/a	n/a
	ss + as N–C	2231	2225	s/n	s/n	n/a	n/a	n/a	n/a

<sup>a</sup> s/n: signal-to-noise too low. n/p: not present. n/a: nonapplicable.

<sup>b</sup> According to studies on cyanamide.

contain peaks corresponding to the asymmetric and symmetric C≡N vibrations (as C≡N and ss C≡N) and a combination band of the symmetric and asymmetric N–C (single bond) stretching modes (ss + as N–C). Finally, the vibration at 2160 cm<sup>-1</sup>, which was found to be present in the dicyanamide salts of divalent metals such as mercury and lead, is possibly due to the formation of isonitrile moieties, which were thought to exist in previous IR studies of cyanamide.<sup>51</sup> A summary of the vibrational modes is shown in Table 1.<sup>52–54</sup>

Spectra for the cation are shown in Figure 5 for polarizations ssp, ppp, sps, and pss. The ssp combination contains the d<sup>+</sup>, d<sup>-</sup>, r<sup>+</sup>, and r<sup>+</sup><sub>FR</sub> vibrations. The C<sub>4</sub>–C<sub>5</sub> ring vibrations appear as very weak bands, located at ~3150 and ~3190 cm<sup>-1</sup> for the antisymmetric and symmetric bands, respectively. The ppp polarization combination shows contributions from d<sup>+</sup>, d<sup>-</sup>, and d<sup>+</sup><sub>FR</sub> and the ring mode vibrations. The sps and pss polarization combinations contain d<sup>+</sup>, d<sup>-</sup>, and antisymmetric methyl stretch (r<sup>-</sup>) vibrations.

**[BMIM][MS].** In this case the vibrational frequencies of both ionic species are located in the same range (2750–3300 cm<sup>-1</sup>). Spectra for the four above-mentioned polarizations are shown in Figure 6. Peaks for d<sup>+</sup>, d<sup>-</sup>, r<sup>+</sup>, and r<sup>+</sup><sub>FR</sub> and the ring modes are visible. The ppp combination shows d<sup>+</sup>, d<sup>-</sup>, r<sup>+</sup>, and r<sup>-</sup> modes. The sps and pss combinations show the r<sup>-</sup> and d<sup>-</sup> modes. The peak corresponding to the symmetric methyl stretch corresponding to the methyl sulfate anion, whose frequency corresponds to 2830 cm<sup>-1</sup>,<sup>55,56</sup> was not discernible in any of the polarization combinations.

**Contact Angle.** The contact angle measurement results are shown in Figure 7. [BMIM][MS] shows a contact angle of 23

± 0.8°, and [BMIM][DCA] shows an angle of 30 ± 0.7°. It is evident that the two compounds wet the surface of the TiO<sub>2</sub> film.

## Discussion

The results from the orientation calculations at the [BMIM]-[MS]/TiO<sub>2</sub> interface are shown in Figure 8. The orientation curves have been plotted as the ratio of amplitudes corresponding to ssp methyl symmetric stretch/sps methyl asymmetric stretch, versus the tilt angle  $\theta$  with respect to the laboratory surface normal, and as a function of the distribution width,  $\sigma$ . The C<sub>3</sub> axis from the terminal methyl in the butyl chain in [BMIM]<sup>+</sup> shows a tilt ranging from 56 to 66° (average of 59°) for values of  $\sigma$  between 0 and 10°. The simulation curves for [BMIM][DCA]/TiO<sub>2</sub> interface are shown in Figure 9a,b for the cation and the anion. For the CH region, the curves show the ratio of ssp methyl symmetric stretch/sps methyl asymmetric stretch versus the tilt angle  $\theta$ . The simulation corresponding to the C≡N stretch presents the ratio of ssp [DCA]<sup>-</sup> symmetric stretch/sps [DCA]<sup>-</sup> asymmetric stretch versus the tilt angle  $\theta$ . The C<sub>3</sub> axis of the methyl group shows a tilt ranging from 68 to 83° (average of 72°), for values of  $\sigma$  between 0 and 10°, while the tilt of the C<sub>2</sub> axis in the dicyanamide anion has an angle that varies between 50 and 63° (average of 53°) for twist angles  $\phi$  ranging from 0 to 40°. The tilt angles of the terminal methyl are comparable to those from [BMIM]<sup>+</sup>-based ionic liquids (tetrafluoroborate and hexafluorophosphate) found in a previous study from Romero et al. on the ionic liquid/hydrophilic SiO<sub>2</sub> interface.<sup>57</sup> In that study, the butyl chain terminal methyl group of [BMIM]<sup>+</sup> shows tilt angles of 78–90° for [BMIM]-[BF<sub>4</sub>] and 58–64° for [BMIM][PF<sub>6</sub>]. There is also agreement with tilt values in the work of Rollins et al. for a similar interface, where the reported tilts for [BMIM][BF<sub>4</sub>] and [BMIM][PF<sub>6</sub>] are 57 and 46°, respectively.<sup>58</sup> There is however a limitation in the evaluation of the distribution, since the surface roughness was not taken into account. In the work of Simpson et al.<sup>59</sup> a method of correction for surface roughness is discussed that uses fractal analysis of AFM micrographs and linear dichroism measurements for the evaluation of the corrected linear dichroism.

The SFG spectra of [BMIM]<sup>+</sup> at the titanium dioxide interface display a large contribution from methylene vibrations (d<sup>+</sup> and d<sup>-</sup>) of the butyl chain in the cation. In both cases, the symmetric and asymmetric vibrations are detected in the ssp spectra, among which the symmetric stretch peak is unusually intense with higher amplitude compared to all other vibrational modes, as opposed to that found in previous investigations on the ionic

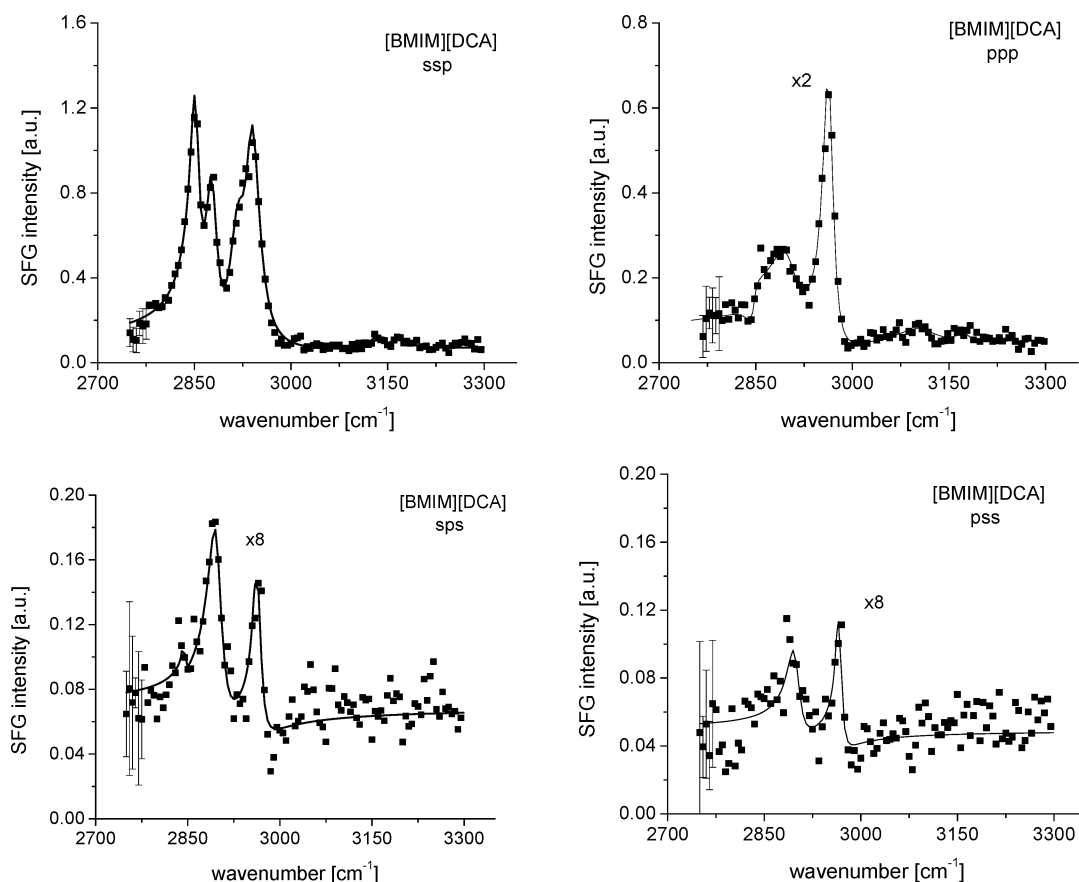


**Figure 5.** SFG spectra of [BMIM][DCA]/TiO<sub>2</sub> interface in the CH stretch region for polarizations ssp, ppp, sps, and pss. Note that the last three plots have been rescaled several times.

liquid/silica interface.<sup>57,58</sup> In the sps and pss polarizations there is also an intense contribution from the d<sup>+</sup> mode. The presence of such vibrational modes is an indication of disorder in the alkyl chains due to the presence of kinks, which cause a break in the centrosymmetry within the trans extended linear carbon chain that otherwise leads to the near cancellation of the methylene contributions.<sup>60,61</sup> The detection of gauche defects in this investigation differs with previous SFG results on the liquid–solid interface. The work of Romero et al.<sup>57,62</sup> on the ionic liquid/solid interface for hydrophilic and hydrophobic silica in [BMIM][BF<sub>4</sub>] and [BMIM][PF<sub>6</sub>] does not show contributions from methylene groups. Similar results were found in the work by Fitchett et al.<sup>63</sup> and Rollins et al.<sup>58</sup> for imidazolium-type ionic liquids based on BF<sub>4</sub><sup>-</sup>, PF<sub>6</sub><sup>-</sup>, and bis(perfluoroalkylsulfonyl)-imide anions, also at the silica surface. The dissimilarity in the results might arise from a difference in the surface roughness. The silica surface used on the aforementioned work is mirrorlike polished, whereas the TiO<sub>2</sub> used in this investigation is constituted by particles of approximately 2.5 nm in diameter, conferring a greater degree of roughness to the surface. Some researchers have used SFG to probe organic adsorbates at the surface of nanoparticles, among which the work of Weeraman et al.<sup>64</sup> and Holman et al.<sup>65</sup> on thiols and arachidate molecules, respectively, suggest that the methylene features in the SFG spectra are due to the roughness of the surface. In addition, the strong methylene contribution can be explained by a less dense packing due to the fact that both ionic species adsorb at the surface, creating a steric hindrance to aggregation and, hence, to favorable Van der Waals interactions.<sup>66</sup>

The surface of silica is usually covered with silanol ( $\equiv\text{Si}-\text{OH}$ ) groups, to which polar molecules tend to adsorb, and for nonaqueous liquids, the adsorption is believed to be largely

influenced by the formation of hydrogen bonds between the silanol groups and electronegative atoms,  $\pi$ -electrons, or charges.<sup>67,68</sup> The structure of titanium dioxide presents a similar case. The surface of the oxide contains titanol ( $\equiv\text{Ti}-\text{OH}$ ) moieties, which are formed when TiO<sub>2</sub> is put in contact with water, forming a surface with varying amounts of hydroxyl groups. These species are formed when water is adsorbed dissociatively as OH<sup>-</sup> and H<sup>+</sup> to satisfy the coordinative unsaturation of the metal, and the surface ions become coordinatively saturated and are then less able to adsorb other molecules. Such a hydroxylated surface needs temperatures of at least 500 K or ion sputtering to remove the hydroxyl groups.<sup>69–72</sup> It is then reasonable to assume that the TiO<sub>2</sub>-coated window used in the present investigation has a surface covered with a certain amount of titanol groups since it has been exposed to water prior to the start of the experiment. In the above-mentioned work by Romero et al., the imidazolium ring is believed to be hydrogen bonded to the quartz surface through both ring nitrogen atoms. In addition, there may exist hydrogen-bonding interactions between the surface hydroxyl groups and the  $\pi$  orbitals of the aromatic ring, which is expected to be nearly parallel to the quartz surface.<sup>57</sup> This was also proposed by Rollins et al. for a number of ionic liquids on the basis of the imidazolium cation.<sup>58</sup> In the present investigation, the SFG peaks corresponding to the ring vibrations are too weak to enable orientation calculations, but their low amplitudes suggest that the imidazolium ring is nearly parallel to the surface of the oxide. This seems in accordance with the ionic liquid's relatively high ability to wet the TiO<sub>2</sub> film, as proved by the contact angle measurements for both compounds. This suggests that it is the positively charged cation ring which exerts a stronger influence on the adsorption to the surface, as compared to the butyl chain,

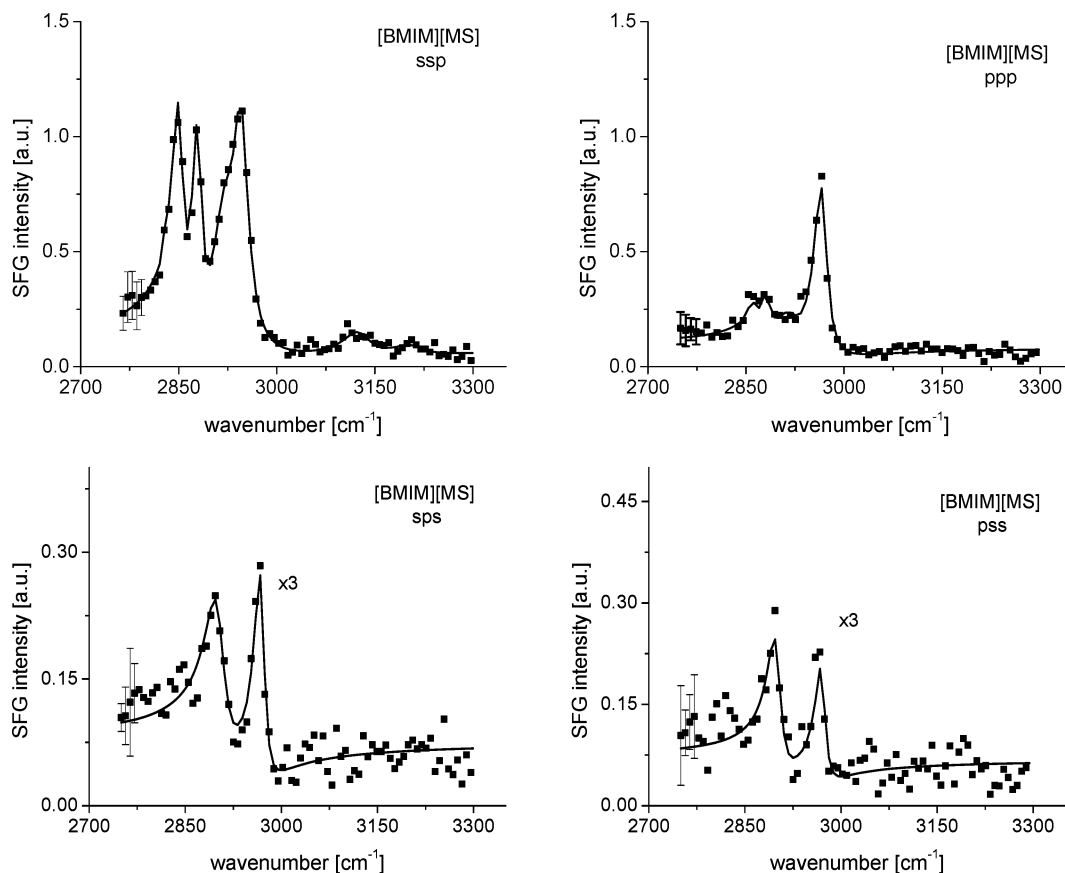


**Figure 6.** SFG spectra of [BMIM][MS]/TiO<sub>2</sub> interface in the CH stretch region for polarizations ssp, ppp, sps, and pss.

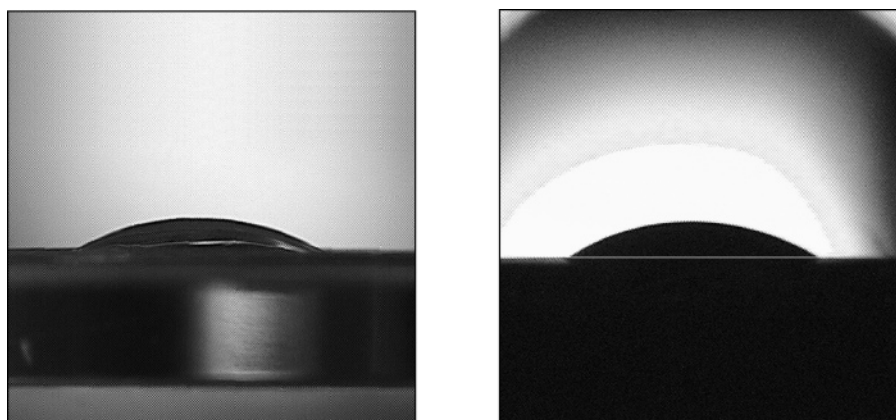


**Figure 7.** Contact angle on the surface of a titanium dioxide film: [BMIM][MS] (left); [BMIM][DCA] (right).

supporting the idea that ion–dipole interactions are stronger than dipole–dipole interactions.<sup>73,74</sup> In addition, previous contact angle studies of imidazolium-based ionic liquids on highly hydrophobic surfaces, such as compressed solid lubricants and functionalized silicon<sup>75</sup> and hydrophobic SiO<sub>2</sub>,<sup>62</sup> show large contact angles. Conversely, studies in glass and metals show angles comparable to those found in this work,<sup>76</sup> highlighting the fact that ionic liquids are polar solvents due to their intrinsic charge density, even though they retain some hydrophobic properties.<sup>77,78</sup>

It is known that dicyanamide possesses Lewis base properties<sup>79–81</sup> and is an efficient coordinating base for transition metals through either the nitrile or amide nitrogens.<sup>82–85</sup> It would be expected that this anion will tend to bind to titanium sites at the surface of TiO<sub>2</sub>. This seems to be the case, as the higher surface concentration of [DCA]<sup>−</sup> compared to [MS]<sup>−</sup> is suggested by the unusually strong SFG signal generated in the C≡N stretch

region (Figure 4). The dicyanamide anion produces well-defined peaks with relatively high signal-to-noise, whereas methyl sulfate does not generate any clearly discernible peak in the SFG spectra, as shown in Figure 6. Similar strong adsorption of dicyanamide was proposed in a previous study of the [BMIM]-[DCA]/platinum interface, where very strong SFG signal from the anion was observed and strong methylene vibrations (d<sup>+</sup>) were found in the potential dependent spectra for positive surface charge excesses. In that investigation, electrochemical measurements suggested that [DCA]<sup>−</sup> forms a multilayer at the surface of platinum metal.<sup>34</sup> In contrast, previous experiments at the [BMIM][MS]/platinum interface performed in this research group showed barely discernible peaks originating from the methyl sulfate anion at different surface charge values.

Approximate calculations of the titania surface charge density (*q*) in contact with the ionic liquids were carried out using the method of Janssens-Maenhout and Schulenberg, initially derived

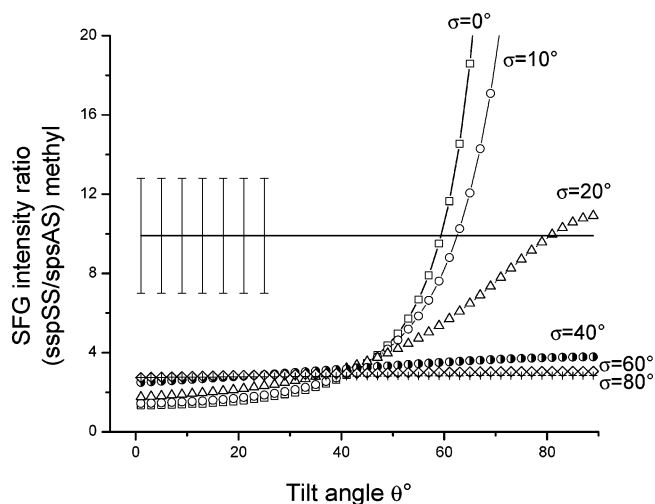


**Figure 8.** Orientation curves for [BMIM][MS] showing the tilt angle  $\theta$  versus the ratio of amplitudes of SFG intensity (ssp SS/spsAS) and as a function of the distribution  $\sigma$ . The solid line represents the experimental ratio value, plotted with error bars, at two standard deviations.

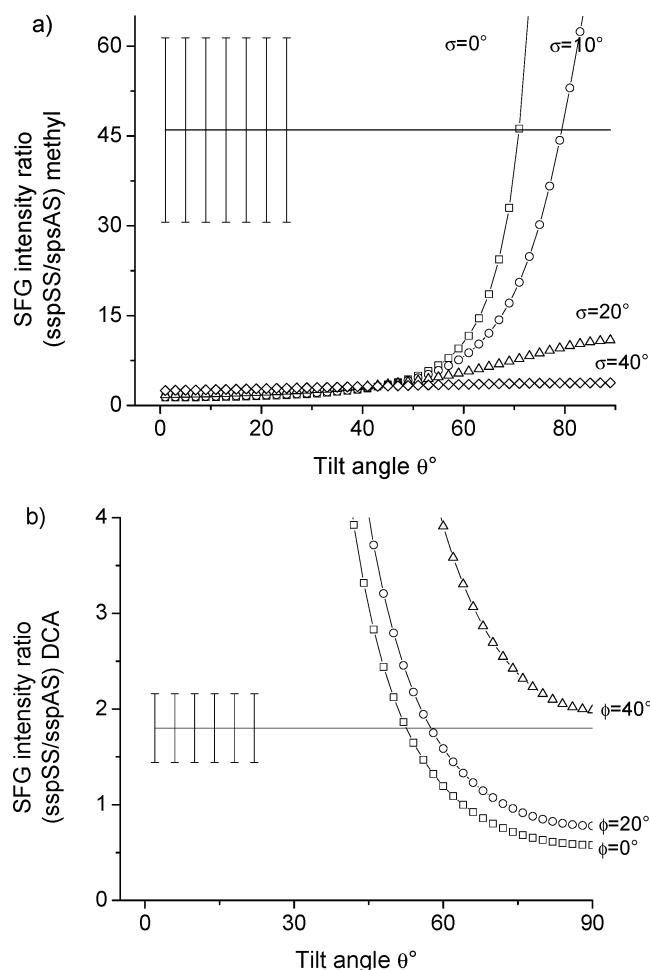


**Figure 9.** Orientation curves for [BMIM][DCA] in (a) the CH region, showing the dependence with the distribution  $\sigma$ , and (b) the CN region, showing the dependence with the twist angle  $\phi$ . The solid line represents the experimental ratio value, plotted with error bars, at two standard deviations.

for electrolytic solutions.<sup>86</sup> A correction factor for the Debye length devised by Smagala et al.<sup>87</sup> is used to account for the effects of ion size, which limits the approaching distance to the charged surface. In dilute solutions the Debye lengths (ap-

proximately 1 nm for 0.1 M solution) extend deep enough into the liquid bulk but drop very quickly as the concentration increases, which is the case of ionic liquids, as described by Rollins et al.<sup>58</sup> The surface charge can be calculated from

$$q = \frac{2\gamma_0}{\rho_0} \left[ \cos \Theta + 1 + \frac{4nkT}{\kappa\gamma_0} \left( \cosh\left(\frac{ze}{2kT} \rho_0\right) - 1 \right) \right] \quad (3)$$

where  $\Theta$  is the contact angle,  $n$  is the bulk concentration in mol/m<sup>3</sup>,  $\gamma_0$  is the surface tension in N/m,  $e$  is the electron charge in C,  $z$  is the charge of the ions,  $\kappa$  is the inverse Debye length in 1/m, and  $\rho_0$  is the surface electrical double layer (EDL) potential defined by

$$\rho_0 = \frac{2kT}{ze} \arcsin h\left(\frac{\kappa q}{4zen}\right) \quad (4)$$

The values of  $q$  for [BMIM][MS] and [BMIM][DCA] were found to be  $60.4 \pm 0.15$  and  $64.4 \pm 0.20$  mC/m<sup>2</sup>, respectively. The calculated  $q$  values are similar to those reported by Rollins et al. for butylimidazolium-based ionic liquids combined with BF<sub>4</sub><sup>-</sup> and PF<sub>6</sub><sup>-</sup> anions. The charge values for the imide-based compounds are substantially lower.<sup>58</sup>

The negative surface charge density for [BMIM][DCA] is higher, which may be explained by a strong specific adsorption of the dicyanamide ions, which increases the negative charge at the interface. The modification of the surface charge density due to specifically adsorbed species has been observed on other systems such as self-assembled monolayers on gold and polymers adsorbed on dielectric surfaces.<sup>88,89</sup> Studies on the adsorption of ionic species with weakly solvated ions such as Cl<sup>-</sup>, Br<sup>-</sup>, I<sup>-</sup>, and SO<sub>4</sub><sup>2-</sup> also revealed the possibility of direct chemical bond formation with the metal surface, resulting in specific adsorption, which significantly affects the electrochemical properties of metal electrodes. A similar specific adsorption is suggested for dicyanamide, since its combination with metals such as copper and silver yields compounds named as pseudohalides.<sup>90</sup> These characteristics may also explain the stronger sum frequency signal generated by the anion in this system.

The surface charge difference of 7% on comparison of methyl sulfate to dicyanamide is significant. This difference corresponds to potential difference of about 30 mV and a Boltzmann factor of 10<sup>6</sup>. Thus, if we had an equal mixture of [BMIM][DCA] and [BMIM][MS], assuming similar double layer thickness of 25 Å (as estimated from electrochemistry and Stark shift data) and ideal mixing behavior, the [DCA] would partition to the surface in excess of [MS]. This is our interpretation of the contact angle and surface charge data. We consider this to be only an estimate in light of above approximations and the fact that the theory is derived from Debye–Hückel and Gouy–Chapman theory and unlikely to be quantitative for these ionic liquids, where the theories are no longer valid.

The surface charge density and the strong SFG signal from [DCA]<sup>-</sup> present the view that the ionic liquids have an extraordinary interaction with the interface. This high degree of association could be the origin of the why ionic liquids display improved performance in dye-sensitized solar cells. The ability of the ionic liquids to effectively screen charge is demonstrated in the simulation works of Lynden-Bell<sup>26</sup> and Madden<sup>25</sup> and the performance of Gratzel cell<sup>91–94</sup> and by these and previous SFG/electrochemical experiments.<sup>95–97</sup> The development of improved performance ionic liquid will be aided with the molecular-level results presented here as a guide.

## Conclusions

The ionic liquid/TiO<sub>2</sub> interface was probed by SFG vibrational spectroscopy for the ionic liquids [BMIM][DCA] and [BMIM][MS]. The presence of both ionic species was detected at the interface for [BMIM][DCA], while only the cation was detectable for [BMIM][MS]. The presence of strong contribution from the methylene vibrations in the SFG spectra is possibly due to the roughness of the surface. Orientation calculations were performed for the ions at the surface, and it was found that the cation's butyl chain shows a range of orientations from 57 to 66° from the surface normal for [BMIM][MS] and from 68 to 83° for [BMIM][DCA]. The C<sub>2</sub> axis from the dicyanamide anion tilts at an angle of 57–73° as a function of the twist, and it is suggested that the anion adsorbs strongly and in an ordered fashion. No calculation results were obtained for the methyl group from [MS]<sup>−</sup> due to its weak SFG signal.

**Acknowledgment.** We are grateful for support from the Welch foundation (Grant E1531). We also thank Nkeng Asong from the M. J. Shultz group at Tufts University for the preparation of the CaF<sub>2</sub>-supported TiO<sub>2</sub> films and Imee Martinez for the assistance in the measurement of the contact angles.

## References and Notes

- (1) Shiro, S.; Yo, K.; Hajime, M.; Yasutaka, O.; Akira, U.; Yuichi, M.; Nobuo, K.; Masayoshi, W.; Nobuyuki, T. *J. Phys. Chem. B* **2006**, *110*, 10228–10230.
- (2) Garcia, B.; Lavalley, S.; Perron, G.; Michot, C.; Armand, M. *Electrochim. Acta* **2004**, *49*, 4583.
- (3) Shin, J.-H.; Henderson, W.; Passerini, S. *J. Electrochem. Soc.* **2005**, *152*, A978.
- (4) Seki, S.; Ohno, Y.; Kobayashi, Y.; Miyashiro, H.; Usami, A.; Mita, Y.; Tokuda, H.; Watanabe, M.; Hayamizu, K.; Tsusuki, S.; Hattori, M.; Terada, N. *J. Electrochem. Soc.* **2007**, *154*, A173.
- (5) Susan, M. A. B. H.; Noda, A.; Mitsushima, S.; Watanabe, M. *Chem. Commun.* **2003**, 938.
- (6) Belieres, J.-P.; Gervasio, D.; Angell, C. A. *Chem. Commun.* **2006**, 4799.
- (7) Ue, M.; Takeda, M.; Toriumi, A.; Kominato, A.; Hagiwara, R.; Ito, Y. *J. Electrochem. Soc.* **2003**, *150*, A499.
- (8) Lewandowski, A.; Galinski, M. *J. Phys. Chem. Solids* **2004**, *65*, 281.
- (9) Shiraishi, S.; Nishina, N.; Oya, A.; Hagiwara, R. *Electrochemistry* **2005**, *73*, 593.
- (10) Galinski, M.; Krajewski, S. R. *Bulg. Chem. Commun.* **2006**, *38*, 192.
- (11) Ohno, H. *Electrochemical Aspects of Ionic Liquids*, 1st ed.; John Wiley and Sons: New York, 2005.
- (12) Fabregat-Santiago, F.; Bisquert, J.; Palomares, E.; Otero, L.; Kuang, D.; Zakeeruddin, S. M.; Gratzel, M. *J. Phys. Chem. C* **2007**, *111*, 6550.
- (13) Fei, Z.; Kuang, D.; Zhao, D.; Klein, C.; Han Ang, W.; Zakeeruddin, S. M.; Gratzel, M.; Dyson, P. J. *Inorg. Chem.* **2006**, *45*, 10407.
- (14) Kuang, D.; Wang, P.; Ito, S.; Zakeeruddin, S. M.; Gratzel, M. *J. Am. Chem. Soc.* **2006**, *128*, 7732.
- (15) Wang, P.; Zakeeruddin, S. M.; Moser, J.-E.; Gratzel, M. *J. Phys. Chem. B* **2003**, *107*, 13280.
- (16) Yamanaka, N.; Kawano, R.; Kubo, W.; Masaki, N.; Kitamura, T.; Wada, Y.; Watanabe, M.; Yanagida, S. *J. Phys. Chem. B* **2007**, ASAP article.
- (17) O'Regan, B.; Gratzel, M. *Nature* **1991**, *353*, 737.
- (18) Bach, U.; Lupo, D.; Comte, P.; Moser, J. E.; Weissortels, F.; Salbeck, J.; Spreitzer, H.; Gratzel, M. *Nature* **1998**, *395*, 583.
- (19) Gratzel, M. *Nature* **2001**, *414*, 338.
- (20) Wang, P.; Zakeeruddin, S. M.; Moser, J. E.; Nazeeruddin, M. K.; Sekiguchi, T.; Gratzel, M. *Nat. Mater.* **2003**, *2*, 402.
- (21) Kambe, S.; Nakade, S.; Kitamura, T.; Wada, Y.; Yanagida, S. *J. Phys. Chem. B* **2002**, *106*, 2967.
- (22) Kubo, W.; Kambe, S.; Nakade, S.; Kitamura, T.; Hanabusa, K.; Wada, Y.; Yanagida, S. *J. Phys. Chem. B* **2003**, *107*, 4374.
- (23) Mazille, F.; Fei, Z.; Kuang, D.; Zhao, D.; Zakeeruddin, S. M.; Gratzel, M.; Dyson, P. J. *Inorg. Chem.* **2006**, *45*, 1585.
- (24) Kawano, R.; Matsui, H.; Matsuyama, C.; Sato, A.; Susan, M. A. B. H.; Tanabe, N.; Watanabe, M. *J. Photochem. Photobiol., A: Chem.* **2004**, *164*, 87.
- (25) Lanning, O. J.; Madden, P. A. *J. Phys. Chem. B* **2004**, *108*, 11069.
- (26) Pinilla, C.; Popolo, M. G.; Kohanoff, J.; Lynden-Bell, R. M. *J. Phys. Chem. B* **2007**, *111*, 4877.
- (27) Shen, Y. R. *The Principles of Nonlinear Optics*; John Wiley and Sons: New York, Chichester, Brisbane, Toronto, Singapore, 1984.
- (28) Buck, M.; Himmelhaus, M. *J. Vac. Sci. Technol., A* **2001**, *19*, 2717.
- (29) Bloembergen, N. *Nonlinear Optics*; W. A. Benjamin Inc.: New York, Amsterdam, 1965.
- (30) Golding, J.; Forsyth, S.; MacFarlane, D. R.; Forsyth, M.; Deacon, G. B. *Green Chem.* **2002**, *4*, 223.
- (31) MacFarlane, D. R.; Golding, J.; Forsyth, S.; Forsyth, M.; Deacon, G. B. *Chem. Commun.* **2001**, 1430.
- (32) Bonhote, P.; Dias, A.-P.; Papageorgiou, N.; Kalayiasundaram, K.; Gratzel, M. *Inorg. Chem.* **1996**, *35*, 1168.
- (33) Holbrey, J. D.; Reichert, W. M.; Swatloski, R. P.; Broker, G. A.; Pittner, W. R.; Seddon, K. R.; Rogers, R. D. *Green Chem.* **2002**, *4*, 407.
- (34) Aliaga, C.; Baldelli, S. *J. Phys. Chem. B* **2006**, *110*, 18481.
- (35) Santos, C.; Rivera-Rubero, S.; Dibrov, S.; Baldelli, S. *J. Phys. Chem. C* **2007**, *111*, 7682.
- (36) Wang, C.-Y.; Groenzin, H.; Shultz, M. J. *J. Phys. Chem. B* **2004**, *108*, 265.
- (37) Wang, C.-Y.; Groenzin, H.; Shultz, M. J. *Langmuir* **2003**, *19*, 7330.
- (38) Wang, R.; Hashimoto, K.; Fujishima, A.; Chikuni, M.; Kojima, E.; Kitamura, A.; Shimohigoshi, M.; Watanabe, T. *Nature* **1997**, *388*, 431.
- (39) Heller, A. *Acc. Chem. Res.* **1995**, *28*, 503.
- (40) Romeas, V.; Pichat, P.; Guillard, C.; Chopin, T.; Lehaut, C. *New J. Chem.* **1999**, *23*, 365.
- (41) Zubkov, T.; Stahl, D.; Thompson, T. L.; Panayotov, D.; Diwald, O.; Yates, J. T. *J. Phys. Chem. B* **2005**, *109*, 15454.
- (42) Stalder, A.; Kulik, G.; Sage, D.; Barbieri, L.; Hoffman, P. *Colloids Surf., A* **2006**, *286*, 92.
- (43) Hirose, C.; Akamatsu, N.; Domen, K. *Appl. Spectrosc.* **1992**, *46*, 1051.
- (44) Hirose, C.; Akamatsu, N.; Domen, K. *J. Chem. Phys.* **1992**, *96*, 997.
- (45) Hirose, C.; Yamamoto, H.; Akamatsu, N.; Domen, K. *J. Phys. Chem.* **1993**, *97*, 10064.
- (46) Wang, H.-F.; Lu, R.; Gan, W.; Wu, B.-H.; Chen, H. *J. Phys. Chem. B* **2004**, *108*, 7297.
- (47) Wang, H.-F.; Lu, R.; Gan, W.; Wu, B.-H.; Zhang, Z.; Guo, Y. *Int. Rev. Phys. Chem.* **2005**, *24*, 191.
- (48) Aliaga, C.; Baldelli, S. *J. Phys. Chem. B* **2007**, in press.
- (49) Rao, Y.; Tao, Y.-S.; Wang, H.-F. *J. Chem. Phys.* **2003**, *119*, 5226.
- (50) Wang, J.; Paszti, Z.; Even, M. A.; Chen, Z. *J. Am. Chem. Soc.* **2001**, *124*, 7016.
- (51) Davies, M.; Jones, M. J. *Trans. Faraday Soc.* **1958**, *54*, 1454.
- (52) Snyder, R. G. *J. Chem. Phys.* **1965**, *42*, 1744.
- (53) Snyder, R. G.; Strauss, H. L.; Elliger, C. A. *J. Phys. Chem.* **1982**, *86*, 5145.
- (54) MacPhail, R. A.; Strauss, H. L.; Snyder, R. G.; Elliger, C. A. *J. Phys. Chem.* **1984**, *88*, 334.
- (55) Lu, R.; Gan, W.; Wu, B.-H.; Zhang, Z.; Guo, Y.; Wang, H.-F. *J. Phys. Chem. B* **2005**, *109*, 14118.
- (56) Superfine, R.; Huang, J. Y.; Shen, Y. R. *Phys. Rev. Lett.* **1991**, *66*, 1066.
- (57) Romero, C.; Baldelli, S. *J. Phys. Chem. B* **2006**, *110*, 6213.
- (58) Rollins, J. B.; Fitchett, B. D.; Conboy, J. C. *J. Phys. Chem. B* **2007**, *111*, 4990.
- (59) Simpson, G. J.; Rowlen, K. L. *J. Phys. Chem. B* **1999**, *103*, 3800.
- (60) Guyot-Sionnest, P.; Hunt, J. H.; Shen, Y. R. *Phys. Rev. Lett.* **1987**, *59*, 1597.
- (61) Bell, G. R.; Li, Z. X.; Bain, C. D.; Fischer, P.; Duffy, D. C. *J. Phys. Chem. B* **1998**, *102*, 9461.
- (62) Romero, C.; Moore, H. J.; Lee, T., R.; Baldelli, S. *J. Phys. Chem. C* **2007**, *111*, 240.
- (63) Fitchett, B. D.; Conboy, J. C. *J. Phys. Chem. B* **2004**, *108*, 20255.
- (64) Weeraman, C.; Yatawara, A. K.; Bordenyuk, A. N.; Benderskii, A. V. *J. Am. Chem. Soc.* **2006**, *128*, 14244.
- (65) Holman, J.; Ye, S.; Neivandt, D. J.; Davies, P. B. *J. Am. Chem. Soc.* **2004**, *126*, 14322.
- (66) Ward, R. N.; Duffy, D. C.; Davies, P. B.; Bain, C. D. *J. Phys. Chem.* **1994**, *98*, 8536.
- (67) Zaki, M. I.; Hasan, M. A.; Al-Sagheer, F. A.; Pasupulety, L. *Colloids Surf., A* **2001**, *190*, 261.
- (68) Iler, R. K. *The Chemistry of Silica*; John Wiley & Sons Inc.: New York, Chichester, Brisbane, Toronto, 1979.
- (69) Hoffman, M. R.; Martin, S. T.; Choi, W.; Bahnmann, D. W. *Chem. Rev.* **1995**, *95*, 69.
- (70) Nohara, K.; Hidaka, H.; Pelizzetti, E.; Serpone, N. *J. Photochem. Photobiol., A: Chem.* **1997**, *102*, 265.
- (71) Namai, Y.; Matsuoka, O. *J. Phys. Chem. B* **2005**, *109*, 23948.
- (72) Kung, H. H. *Transition Metal Oxides*; Elsevier Science Publishers BV: Amsterdam, Oxford, New York, Tokyo, 1989; Vol. 45.

- (73) Chattoraj, D. K.; Birdi, K. S. *Adsorption and the Gibbs Surface Excess*; Plenum Press: New York, London, 1984.
- (74) Zisman, W. A. *Ind. Eng. Chem.* **1963**, *55*, 18.
- (75) Gao, L.; McCarthy, T. J. *J. Am. Chem. Soc.* **2007**, *129*, 3804.
- (76) Wang, W.; Murray, R. W. *Anal. Chem.* **2007**, *79*, 1213.
- (77) Welton, T. *Chem. Rev.* **1999**, *99*, 2071.
- (78) Dupont, J.; de Souza, R. F.; Suarez, P. A. *Z. Chem. Rev.* **2002**, *102*, 3667.
- (79) Schlueter, J. A.; Geiser, U.; Manson, J. L. *J. Phys.* **2004**, *114*, 475.
- (80) MacFarlane, D. R.; Pringle, J. M.; Johansson, K. M.; Forsyth, S. A.; Forsyth, M. *Chem. Commun.* **2006**, 1905.
- (81) MacFarlane, D. R.; Forsyth, S. A.; Golding, J.; Deacon, G. B. *Green Chem.* **2002**, *4*, 223.
- (82) Potocnak, I.; Dunaj-Jurco, M.; Miklos, D.; Kabesova, M.; Jager, L. *Acta Crystallogr.* **1995**, *C51*, 600.
- (83) Kohler, H.; Wusterhausen, H.; Jeschke, M.; Kolbe, A. *Z. Anorg. Allg. Chem.* **1987**, *547*, 69.
- (84) Kooijman, H.; Spek, A.; Van Albada, G.; Reedijk, J. *Acta Crystallogr.* **2002**, *C58*, m124.
- (85) Karmakar, R.; Choudhury, C. R.; Hughes, D. L.; Yap, G. P. A.; El Fallah, M. S.; Desplanches, C.; Sutter, J.-P.; Mitra, S. *Inorg. Chim. Acta* **2006**, *359*, 1184.
- (86) Janssens-Maenhout, G. G. A.; Schulenberg, T. *J. Colloid Interface Sci.* **2003**, *257*, 141.
- (87) Smagala, T. G.; Fawcett, W. R. *Z. Phys. Chem. (Munich)* **2006**, *220*, 427.
- (88) Joppien, G. R. *J. Phys. Chem.* **1978**, *82*, 2210.
- (89) Tulpar, A.; Ducker, W. A. *J. Phys. Chem. B* **2004**, *108*, 1667.
- (90) Koehler, H.; Jeschke, M.; Kolbe, A. *Z. Chem.* **1985**, *25*, 340.
- (91) Wang, P.; Zakeeruddin, S.; Moser, J.; Humphry, R.; Gratzel, M. *J. Am. Chem. Soc.* **2004**, *126*, 7164.
- (92) Wang, P.; Zakeeruddin, S. M.; Comte, P.; Exnar, I.; Gratzel, M. *J. Am. Chem. Soc.* **2003**, *125*, 1166.
- (93) Wang, P.; Zakeeruddin, S. M.; Moser, J.-E.; Gratzel, M. *J. Phys. Chem. B* **2003**, *107*, 13280.
- (94) Wang, P.; Zakeeruddin, S.; Moser, J.; Gratzel, M. *J. Phys. Chem. B* **2003**, *107*, 13280.
- (95) Aliaga, C.; Baldelli, S. *J. Phys. Chem. B* **2006**, *110*, 18481.
- (96) Baldelli, S. *J. Phys. Chem. B* **2005**, *109*, 13049.
- (97) Rivera-Rubero, S.; Baldelli, S. *J. Phys. Chem. B* **2004**, *108*, 15133.